2015 International Nuclear Atlantic Conference - INAC 2015
São Paulo, SP, Brazil, October 4-9, 2015
ASSOCIAÇÃO BRASILEIRA DE ENERGIA NUCLEAR - ABEN
ISBN: **978-85-99141-06-9**

SYNCHROTRON DIFFRACTION CHARACTERIZATION OF NANOSTRUCTURED KY_3F_{10}:Tb

Rodrigo U. Ichikawa[1], Horacio M. S. M. D. Linhares[2], Maria I. Teixeira[1], Izilda M. Ranieri[1], Xavier Turrillas[3] and Luis G. Martinez[1*]

[1] Instituto de Pesquisas Energéticas e Nucleares (IPEN / CNEN - SP)
Av. Professor Lineu Prestes 2242
05508-000 São Paulo, SP
ichikawa@usp.br, miteixeira@ipen.br, iranieri@ipen.br, *lgallego@ipen.br

[2] Universidade Federal Fluminense (INFES / UFF - RJ)
Avenida João Jasbick, s/nº
28470-000 Santo Antônio de Pádua, RJ
horacio_marconi@yahoo.com.br

[3] Institut de Ciència de Materials de Barcelona (ICMAB / CSIC)
Dept. of Crystallography - UAB Campus
08193 Bellaterra, Spain
turrillas@gmail.com

ABSTRACT

Nanostructured rare-earth fluorides materials are being intensively studied recently due to their potential applications in high-dose dosimetry. Particularly, nanostructured Tb-doped KY_3F_{10} has shown satisfactory results to be used in this area. In the present work, the structure and microstructure of KY_3F_{10}:Tb was investigated by means of X-ray synchrotron diffraction. One of the samples was analyzed as synthesized and another after a heat treatment. Rietveld refinement of synchrotron diffraction data was applied to obtain cell parameters, atomic positions and atomic displacement factors and the results were compared to values found in literature. X-ray line profile analysis methods were applied to determine mean crystallite sizes and their distribution.

1. INTRODUCTION

Nanostructured rare-earth fluorides are being intensively studied. These fluorides are very interesting due to its high transparency, which extends up to infrared, and its low phonon energy. These characteristics decrease the probability of non-radioactive ion transitions, making them suitable to be used in optical applications. Other properties are: high thermal conductivity, good mechanical properties, high chemical stability and high solubility which permits the incorporation of other ions from the same group. Particularly, KY_3F_{10} crystal has been studied as luminescent material when activated by rare-earth ions [1-3].

Linhares [2] studied the synthesis of nanostructured rare-earth doped KY_3F_{10} by co-precipitation technique. This technique was chosen since requires relatively simple and low cost experimental apparatus. Specifically, for Tb-doped KY_3F_{10} nanocrystals (0.4 mol% Tb), thermoluminescence emission (TL) spectra and optically stimulated luminescence (OSL) dose–response results indicate this material as very suitable to be used in high dose radiation dosimetry.

In order to investigate the structure and microstructure of KY_3F_{10}:Tb synchrotron radiation diffraction techniques were employed. X-ray line profile analysis using the Warren-Averbach method was performed to determine the mean crystallite sizes, crystallite sizes distribution and microstrains. The results for mean crystallite sizes were confirmed by transmission electron microscopy [2]. The synchrotron diffraction data were also analyzed by Rietveld refinement in order to study the crystal structure of the material. By the Rietveld refinement of the crystal structure it was determined the cell parameter for the cubic structure, atomic positions and atomic displacement factors.

2. EXPERIMENTAL

The KY_3F_{10} nanocrystals doped with Tb (0.4 mol%) were synthesized by co-precipitation technique in aqueous solution, as described in detail in previous works [1,2].

For the thermoluminescent characterization, a pellet of KY_3F_{10}:Tb/Teflon was produced at the Dosimetric Materials Production Laboratory of IPEN. The pellet of 50 mg, in a proportion of 2 (Teflon) : 1 (KY_3F_{10}) (6 mm diameter; 2 mm thickness) was pressed under 2 tons load. The pellets were irradiated at the Radiation Technology Center of IPEN, using Gamma-Cell 220 - ^{60}Co system (dose rate 1.258 kGy/h), from 0.10 kGy up to 50 kGy doses.

The irradiation was performed at ambient temperature. To ensure electronic balance the sample was mounted in PMMA, poly (methyl methacrylate), plates with 3 mm of thickness and wrapped in aluminum foil.

The thermoluminescence (TL) measurements were performed using an equipment RISÖ TL/OSL Reader and Controller, model DA-20. The TL data acquisition were performed at ambient temperature up to 300 ºC, under constant N_2 flux of 2.5 L/min, with U340 filter and heating rate of 10 °C/s. The optically stimulated luminescence (OSL) measurements were performed in the same equipment, using as light source a set with 28 LED (light emitting diodes) which emits at 470 nm delivering 80 mW/cm^2.

The synchrotron radiation measurements were collected in the MSPD beamline at ALBA Synchrotron Light Source (Barcelona - Spain), with the collaboration of ALBA staff, using the wavelength of 0.41332793 Å. The set up with a MYTHEN II detector provided high counting statistics suitable to perform properly the microstructural and structural analysis.

3. METHODS

3.1. Thermoluminescence (TL) and Optically Stimulated Luminescence (OSL)

High-energy radiation can create excited electronic states in some crystalline materials and these states can be trapped by crystal lattice defects (electron-hole pairs). These states are not energetically stable, but can remain in its metastable state for long times. When enough energy is supplied to the system the trapped states can rapidly decay to low-energy states, causing the emission of light photons.

When the energy for the decay is in the form of heat the phenomenon is called thermoluminescence (TL) [4]. When the decay is promoted by light stimulation the process is called optically stimulated luminescence (OPL).

3.2. X-ray line profile analysis

For the determination of mean crystallite sizes, microstrains and the crystallite sizes distribution, the Warren-Averbach method [5] was used. From the kinematical theory of X-ray diffraction the physical profile of a Bragg reflection is given by the convolution of the crystallite size and the microstrain profiles [6]. The application of Fourier Transform on the physical profile allows separating these two contributions and this method is known as the Bertaut-Warren-Averbach Method or simply Warren-Averbach Method:

$$lnA\left(L,\frac{1}{d}\right) = lnA^S(L) - 2\pi^2\langle {\varepsilon_L}^2\rangle L^2/d^2 \quad (1)$$

where L is the Fourier Length, defined as $L = n.a_3$, where $a_3 = \lambda/2(sin\theta_2 - sin\theta_1)$, n is the harmonic number, θ_1 is the initial angle of the peak, θ_2 is the final angle of the peak, d is the interplanar spacing and $\langle {\varepsilon_L}^2\rangle$ stand for mean squared strain [6].

With the linear equation given by EQ. 1, it is possible to separate size (linear coefficient) and microstrain (slope) contributions from a linear fit. To calculate the mean crystallite sizes, the values of $A^S(L)$ against L were plotted, where the intercept of the initial slope on the L-axis gives the area-weighted column length $\langle L\rangle_{area}$.

The volume-weighted column length ($\langle L\rangle_{vol}$) was also estimated to determine the crystallite size distribution. According to Krill and Birringer [7] the volume-weighted column length can be calculated using EQ. 2, if the normalization $A^S(0)$ is assumed.

$$\int_0^{+\infty} A^S(L)dL = \frac{\langle L\rangle_{vol}}{2} \quad (2)$$

With these two weighted average column lengths and assuming a spherical form for the crystallites (crystallites with diameter$D$) it is possible to determine the crystallite size distribution. A function widely used to describe the distribution of volumetric entities is the lognormal function, given by EQ. 3.

$$g(D) = \frac{1}{\sqrt{2\pi}D\ln\sigma} exp\left\{-\frac{1}{2}\left[\frac{\ln(D/D_0)}{\ln\sigma}\right]^2\right\} \quad (3)$$

$g(D)$ can be calculated by determining the parameters D_0 and σ, also known as median and lognormal variance respectively [8], using $\langle L\rangle_{area}$ and $\langle L\rangle_{vol}$ [7].

The Rietveld refinement method [9-11] of analyzing powder diffraction data is a methodology by which the crystal structure is refined by fitting the entire profile of the diffraction pattern to a calculated profile using a least-squares approach. The Rietveld method requires a starting structural model based on approximate atomic positions and a non-structural model, which describes the Bragg reflections in terms of analytical or other differentiable functions. The main aim of the Rietveld method is to refine the atomic positions using powder diffraction data, also providing estimations of line-profile parameters. The total intensity of reflections and, to a first approximation, their positions, are determined by the structural model, but the shape of the Bragg reflections depends on the instrumental function and on the effects of the microstructure of the sample.

4. RESULTS AND DISCUSSION

The TL emission curves were measured in 0.10 kGy up to 50 kGy range (FIG. 1). The curves present two peaks: one at approximately at 190 ºC which then increases in intensity up to 5 kGy and sharply drops to higher doses (FIG. 1a) and other one at approximately at 250 ºC which proportionally increases in intensity to the irradiation dose. Normalizing the curves it can be seen that the 10kGy curve presents a peak broadening at 258 ºC. The formation of new centers was not observed. The dose-response curve was obtained by area integration beneath the peaks from TL; this curve presents a sub linearity and saturation from 5 kGy.

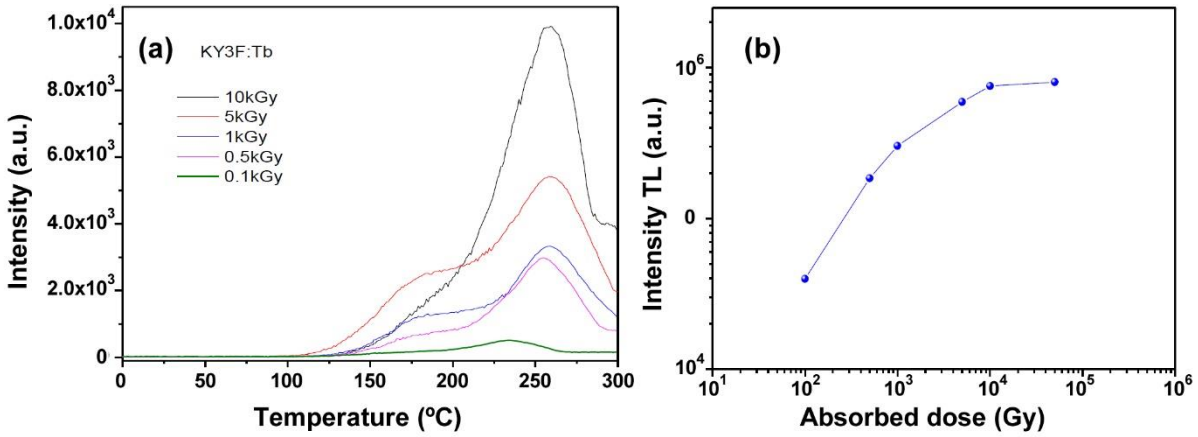

Figure 1: (a) TL emission curves and (b) dose-response curve for KY_3F_{10}:Tb nanocrystal.

The OSL was obtained for two doses to verify if it could be used as alternative to TL, however the signal was not intense when the sample was excited with a diode laser with 470 nm emission. This indicates that the emission was not sufficient to stimulate trapped metastable charges of the defects produced by the radiation.

The minimum detectable dose of the samples was determined by studying the variability of the TL signal obtained from non-irradiated samples. It is defined by the triple calculation of the standard deviation in five measurements of mean doses from the non-irradiated sample. The obtained value was 0.15 Gy. For the determination of the TL reproducibility five samples

submitted five times to the same irradiation procedure using ^{60}Co (1 kGy) and TL reading were used.

The calibration factor of each sample was obtained using the ratio between the absorbed dose value and mean value of its response. The reproducibility of the results in this experience is given by the coefficient of variation (CV%), which is the ratio between the standard deviation and the mean measurement for each sample. The maximum value was 6.56%. A satisfactory result of CV% for the material to be considered as dosimetric is up to 10%, showing that Tb-doped KY_3F_{10} is in the satisfactory range in this aspect.

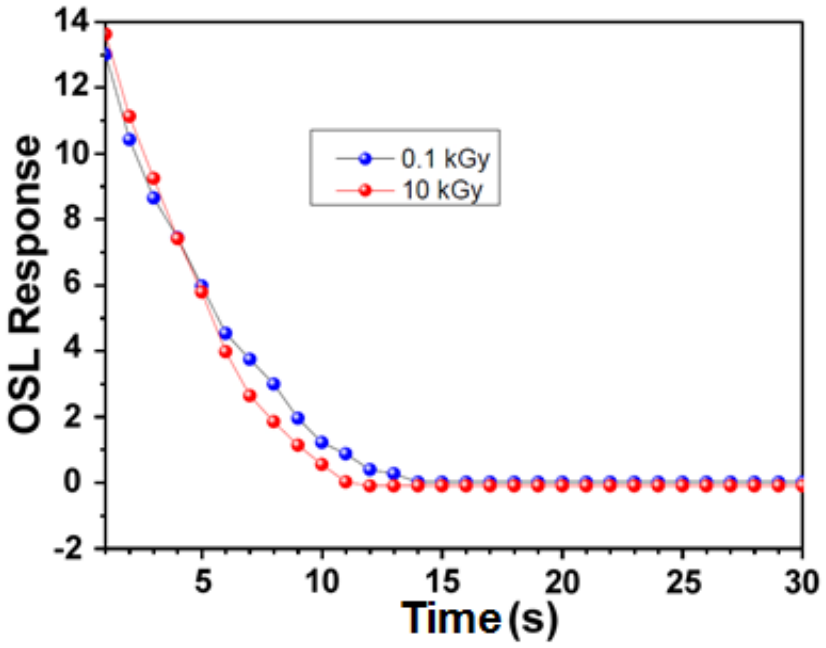

Figure 2: OSL curve for KY_3F_{10}:Tb nanocrystal.

The microstructural characterization was performed first using Warren-Averbach method to determine the area-weighted mean crystallite size, followed by integration of the area under the curve presented in FIG. 3, according to EQ. 2. The X-ray diffraction peaks used in the analysis correspond to (111) and (222) planes. Also, in X-ray line profile analysis is very important to correctly take into account the contribution from the instrument. In this case, Si 640c from NIST was measured to correct the instrumental broadening in the X-ray profiles according to a computer program developed by one of the authors [12].

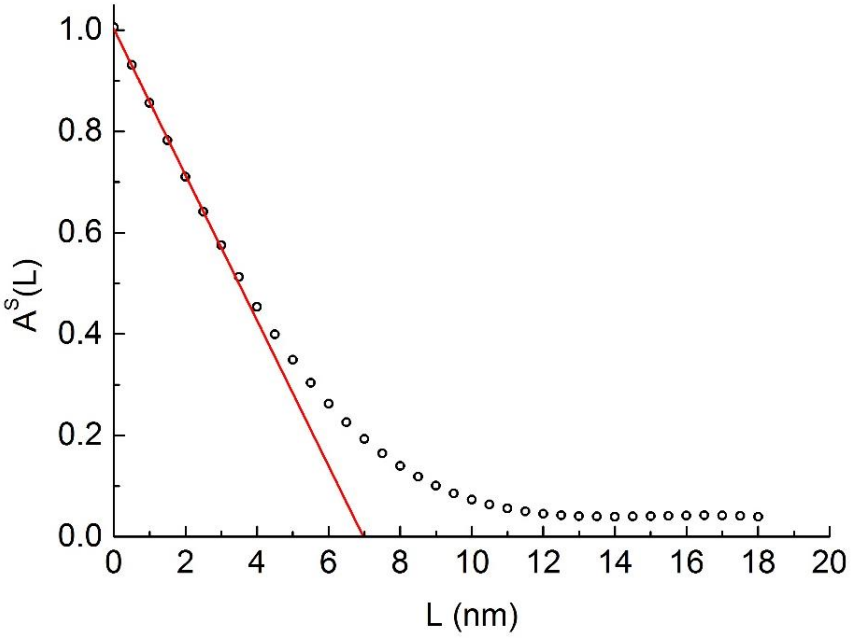

Figure 3: Plot of $A^S(L)$ vs L from Warren-Averbach method. In red: linear extrapolation to determine the area-weighted mean crystallite size.

The crystallite size distribution was determined assuming spherical crystallites. TEM images confirmed the spherical form of the crystallite as presented by Linhares [2]. In FIG. 4 the distribution can be visualized.

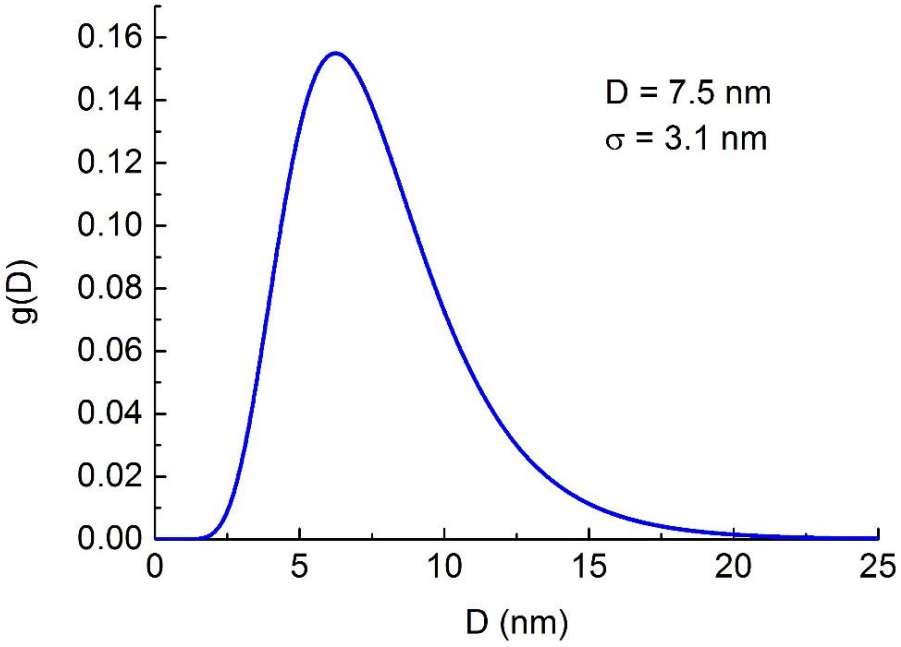

Figure 4: Crystallite size distribution for KY_3F_{10}:Tb nanocrystal.

Table 1: Area ($\langle L \rangle_{area}$), volume-weighted ($\langle L \rangle_{vol}$) mean crystallite sizes and mean crystallite size (D) obtained by the distribution with standard deviation σ

$\langle L \rangle_{area}$ (nm)	$\langle L \rangle_{vol}$ (nm)	D (nm)	σ (nm)
7.0	9.1	7.5	3.1

The root mean square strain presented a negative value for the mean square strain, which can be considered as zero, in other words, a negligible microstrain is presented in the sample. The values presented in TAB. 1 are in very well accordance with TEM images presented in another work by Linhares [2]. The narrow distribution obtained indicates the low size dispersion of the sample.

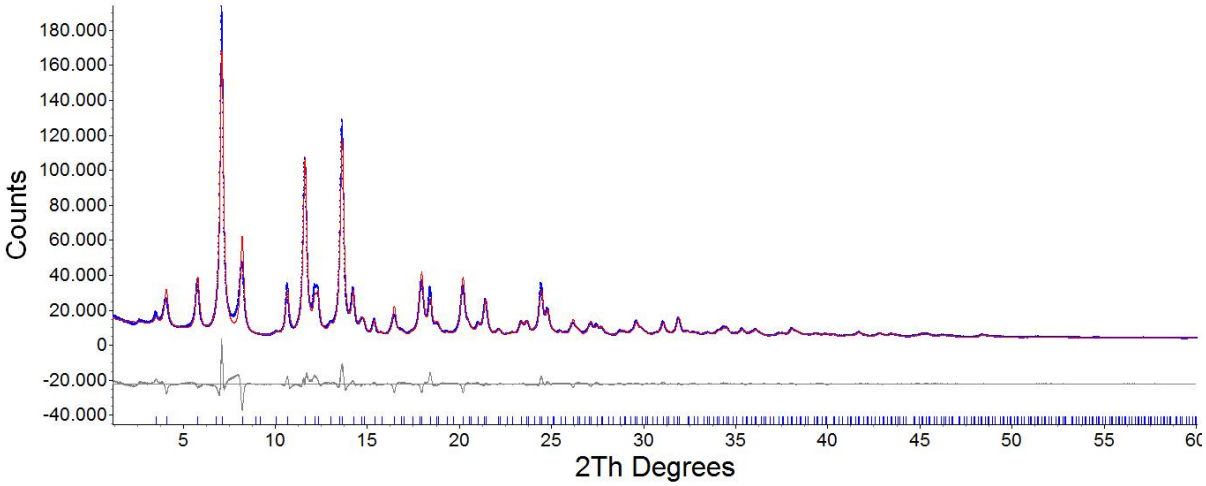

Figure 5: Rietveld refinement for KY_3F_{10}:Tb nanocrystal using synchrotron radiation data.

Lastly, Rietveld refinement was performed to probe the average structure of the material. The model was refined for the cubic space group $Fm\bar{3}m$. ICSD CIF File 409643 was used as reference for the starting values of the refined parameters. In the analysis cell parameters, atomic positions and isotropic atomic displacement parameters were refined. The results are presented in TAB. 2.

Table 2: Rietveld refinement results for cell parameter (a), isotropic atomic displacement factors (Uiso) and atomic positions (x, y, z)

a (Å)	Uiso K (Å²)	Uiso Y (Å²)	Uiso F1 (Å²)	Uiso F2 (Å²)	x_Y	x_{F1}, y_{F1}, z_{F1}	y_{F2}, z_{F2}
11.5474(2)	0.02419(7)	0.00650(5)	0.01118(9)	0.00712(8)	0.24069(7)	0.11327(5)	0.16497(6)

The cubic structure is very well adjusted in the experimental data with Rwp = 6.882%, but some discrepancies can be seen in the fit. At the 7.8° region, where an overlap occurs, the model is not well fitted and the intensities were also not well fitted. Since Rietveld analysis consider the average structure, methods that can probe the local structure and could provide more information about the short range ordering are being planned for complementing the results. The experiments for the application of these methods demand high energy synchrotron radiation and will be submitted as research proposals to third generation synchrotron sources.

5. CONCLUSIONS

Tb-doped KY_3F_{10} doped nanocrystals presented promising results to be used in high dose radiation dosimetry, as showed by its TL properties. X-ray line profile analysis, revealed that nanocrystals with approximately 7.5 nm were obtained with negligible microstrain. Also the crystallite sizes distribution is quite narrow indicating low size dispersion. The cubic model was fitted using Rietveld analysis. Although, some problems at 7.8° region were observed, the model is well adjusted. To complement the structural study, other methods that can probe the local structure are planed be applied to verify the material short range ordering.

ACKNOWLEDGMENTS

The authors acknowledge ALBA Synchrotron Light Source for the synchrotron radiation measurements. R. U. Ichikawa acknowledges CNPq and CAPES for the financial support.

REFERENCES

1. L. Gomes, H. M. S. M. D. Linhares, R. U. Ichikawa, L. G. Martinez, I. M. Ranieri, "Luminescence properties of Yb:Nd:Tm:KY3F10 nanophosphor and thermal treatment effects", *Journal of Luminescence*, **v. 157**, pp.285–292 (2015).
2. H. M. S. M. D. Linhares, "Síntese de nanocristais de KY_3F_{10} pelo método de co-precipitação visando aplicações ópticas", *Tese de Doutorado em Tecnologia Nuclear – Materiais.* Instituto de Pesquisas Energéticas e Nucleares, Universidade de São Paulo, São Paulo (2014).
3. J. Zhang, Z. Hao, X. Zhang, Y. Luo, X. Ren, X. J. Wang, J. Zhang, J., "Color tunable phosphorescence in KY_3F_{10}:Tb^{3+} for X-ray or cathode-ray tubes", *J. Appl. Phys.*, **v. 106**, n.03, pp. 3-8 (2009).
4. A. J. J. Bos, "Theory of Thermoluminescence", Radiation Measurements, **v. 41**, Suppl. 1, pp.45-56 (2006).
5. B. E. Warren, B. L. Averbach, "The Effect of Cold-Work Distortion on X-Ray Patterns", *J. Appl. Phys.*, **v. 21**, pp.595-599 (1950).
6. T. Ungár, J. Gubicza, G. Ribárik, A. Borbély, "Crystallite size distribution and dislocation structure determined by diffraction profile analysis: principles and practical application to cubic and hexagonal crystals", *J. Appl. Cryst.*, **v. 34**, pp.298–310 (2001).
7. C. E. Krill, R. Haberkorn, R. Birringer, "*Specification of Microstructure and Characterization by Scattering Techniques*", In: H. S. Nalwa: "*Handbook of*

Nanostructured Materials and Nanotechnology". V. 2: *Spectroscopy and Theory*. Academic Press. (2000).
8. N. Armstrong, W. Kalceff, J. P. Cline, J. Bonevich, "*A Bayesian/Maximum Entropy Method for the Certification of a Nanocrystallite-Size NIST Standard Reference Material*", In: E. J. Mittemeijer, P. Scardi, *Diffraction Analysis of the Microstructure of Materials*. Springer-Verlag Berlin Heidelberg (2004).
9. H.M. Rietveld," Line profiles of neutron powder-diffraction peaks for structure refinement" *Acta Cryst.* **v. 22**, 151-152 (1967).
10. H.M. Rietveld, "A profile refinement method for nuclear and magnetic structures", *J. Appl. Cryst.*, **v. 2**, 65-71 (1969).
11. R.A. Young (ed.), *The Rietveld Method*, Oxford University Press, New York (1993).
12. R. U. Ichikawa, L. G. Martinez, K. Imakuma, X. Turrillas, "Development of a methodology for the application of the Warren-Averbach method", pp. 107-110 . *In: Anais do V Encontro Científico de Física Aplicada*. Blucher Physics Proceedings, n.1, **v. 1**. São Paulo: Blucher (2014).